The EMBO Journal (2004) 23, 3677–3688 | © 2004 European Molecular Biology Organization | All Rights Reserved 0261-4189/04
www.embojournal.org

THE EMBO JOURNAL

Lats2/Kpm is required for embryonic development, proliferation control and genomic integrity

John Peter McPherson[1,4], Laura Tamblyn[1], Andrew Elia[1], Eva Migon[1], Amro Shehabeldin[1], Elzbieta Matysiak-Zablocki[1], Bénédicte Lemmers[1], Leonardo Salmena[1], Anne Hakem[1], Jason Fish[1], Farah Kassam[1], Jeremy Squire[1], Benoit G Bruneau[2], M Prakash Hande[3] and Razqallah Hakem[1,*]

[1]Division of Cellular & Molecular Biology, Department of Medical Biophysics, Ontario Cancer Institute, University of Toronto, Toronto, Ontario, Canada, [2]Cardiovascular Research and Developmental Biology, The Hospital for Sick Children, Toronto, Ontario, Canada and [3]Faculty of Medicine, Department of Physiology and Oncology Research Institute, National University of Singapore, Singapore

The *Drosophila melanogaster warts/lats* tumour suppressor has two mammalian counterparts *LATS1/Warts-1* and *LATS2/Kpm*. Here, we show that mammalian Lats orthologues exhibit distinct expression profiles according to germ cell layer origin. *Lats2*$^{-/-}$ embryos show overgrowth in restricted tissues of mesodermal lineage; however, lethality ultimately ensues on or before embryonic day 12.5 preceded by defective proliferation. *Lats2*$^{-/-}$ mouse embryonic fibroblasts (MEFs) acquire growth advantages and display a profound defect in contact inhibition of growth, yet exhibit defective cytokinesis. *Lats2*$^{-/-}$ embryos and MEFs display centrosome amplification and genomic instability. Lats2 localizes to centrosomes and overexpression of Lats2 suppresses centrosome overduplication induced in wild-type MEFs and reverses centrosome amplification inherent in *Lats2*$^{-/-}$ MEFs. These findings indicate an essential role of Lats2 in the integrity of processes that govern centrosome duplication, maintenance of mitotic fidelity and genomic stability.

The EMBO Journal (2004) **23,** 3677–3688. doi:10.1038/sj.emboj.7600371; Published online 2 September 2004
Subject Categories: genome stability & dynamics; development
Keywords: centrosome; embryonic lethality; genomic instability; Kpm; Lats2

*Corresponding author. Division of Cellular & Molecular Biology, Department of Medical Biophysics, Ontario Cancer Institute, University of Toronto, Suite 706, 620 University Ave., Toronto, Ontario, Canada M5G 2C1. Tel.: +1 416 204 2298; Fax: +1 416 204 2277;
E-mail: rhakem@uhnres.utoronto.ca
[4]Present address: Department of Pharmacology, University of Toronto, Toronto, Ontario, Canada

Received: 13 November 2003; accepted: 27 July 2004; published online: 2 September 2004

Introduction

The equal distribution of duplicated chromosomes to daughter cells is dependent on proper assembly and function of bipolar spindles during mitosis. Checkpoint defects that permit mis-segregation of mitotic chromosomes have the potential of permitting the generation of progeny with improper chromosome numbers and gene dosage (Hartwell and Kastan, 1994). Conditions favouring the continued propagation of cells with unbalanced segregation facilitate neoplastic transformation through the exposure of recessive mutations by loss of heterozygosity. This chromosomal instability phenotype, or aneuploidy, is observed in a majority of tumour cells (Mitelman, 1971).

Several molecular mechanisms have been identified that potentiate chromosomal instability when defective (Hartwell and Kastan, 1994). The generation of aneuploid cells has been proposed to proceed in many cases through a tetraploid intermediate step (Galipeau *et al*, 1996; Borel *et al*, 2002; Meraldi *et al*, 2002) that can arise by the disruption of mitotic chromosomal segregation (Minn *et al*, 1996) or cytokinesis (Andreassen *et al*, 2001). Supernumerary centrosomes that facilitate the generation of multipolar spindles would allow the generation of aneuploid daughter cells through unequal chromosome segregation (Doxsey, 2001; Lange, 2002; Nigg, 2002). Supernumerary centrosomes present in tumour cells have been associated with the formation of multipolar spindles and genomic instability (Lingle *et al*, 1998, 2002; Brinkley, 2001).

The study of components important in developmental control of growth regulation in model organisms such as *Drosophila* has greatly facilitated our understanding of corresponding pathways that are relevant in cancer biology. The *warts* (Bryant *et al*, 1993; Justice *et al*, 1995) or *lats* (Xu *et al*, 1995) gene was originally identified in genetic screens designed to identify mutations that result in tissue overgrowth in *Drosophila*. Warts/Lats is a serine–threonine kinase that is structurally related to proteins that regulate mitotic exit or septation initiation in *Saccharomyces cerevisiae* and *Schizosaccharomyces pombe*, respectively (Nigg, 2001). Embryonic lethality and overproliferation in *lats* mutant flies were suppressed by reducing *cdc2* or *cyclin A* gene dosage (Tao *et al*, 1999). Excessive cyclin A/cdk1 activity in the absence of *lats* was proposed to contribute to the excessive overgrowth that appears in *warts/lats* mutant cells. However, cell cycle deregulation as a sole mechanism of overgrowth has not been supported by other studies (Weinkove and Leevers, 2000). *sav* has been shown to cooperate with *warts/lats* in a novel pathway that simultaneously impacts control of cell death and proliferation (Tapon *et al*, 2002). Cells mutant for either *warts/lats* or *sav* were found to exhibit delays in cell cycle exit and diminished apoptosis, which were attributed to elevated levels of cyclin E and DIAP1 levels, respectively.

Mammalian orthologues of *sav* and *warts/lats* have been implicated in the regulation of cell cycle progression and tumour suppression. Mutations in a human homologue of *sav* (*hWW45*) were identified in three cancer cell lines (Tapon *et al*, 2002). Two mammalian orthologues of *warts/lats* have been identified in mammals: *LATS1/Warts-1* (Nishiyama *et al*, 1999; Tao *et al*, 1999) and *LATS2/Kpm* (Hori *et al*, 2000; Yabuta *et al*, 2000). LATS1/Warts-1 protein is phosphorylated during the M phase of the cell cycle, colocalizes with centrosomes and the mitotic spindle, and associates with Cdk1 and Zyxin (Nishiyama *et al*, 1999; Tao *et al*, 1999; Hirota *et al*, 2000). Mice mutant for *Lats1* developed pituitary hyperplasia and were susceptible to sarcomas and ovarian cancer (St John *et al*, 1999). However, hyperplasia and tumour development were observed in a restricted number of tissues in these mice, compared to the overgrowth phenotype observed in a wide range of tissues and developmental stages of *warts/lats* mutant flies. Hence, Lats1 might not encompass the entire mammalian equivalent of *warts/lats* activity.

Despite structural similarities and similar M-phase phosphorylation (Hori *et al*, 2000; Yabuta *et al*, 2000), the biological role of LATS2/kpm remains unknown. Conflicting results have been reported describing the effects of LATS2/kpm on cell cycle progression, in that LATS2/kpm overexpression has been described to result in a G2/M-phase arrest and apoptosis (Kamikubo *et al*, 2003) or inhibition of the G1–S transition (Li *et al*, 2003).

In order to clarify the biological function of LATS2/kpm, we have generated mice that carry a targeted mutation of the *Lats2* locus. In this study, we show that *lats/warts* orthologues display distinct expression profiles according to germ cell layer origin. Furthermore, we show that disruption of *Lats2* exerts contrasting roles in proliferation depending on the cellular context. Although $Lats2^{-/-}$ embryos exhibit an arrest in proliferation prior to embryonic lethality, $Lats2^{-/-}$ mouse embryonic fibroblasts (MEFs) acquire growth advantages that appear to be strikingly similar to those of mutant *warts/lats* cells in *Drosophila*. We also show that Lats2 is a centrosomal protein that negatively regulates centrosome duplication. $Lats2^{-/-}$ embryonic cells exhibit an increased frequency of cytokinesis defects, micronuclei accumulation, supernumerary centrosomes and aneuploidy, suggesting a role for *Lats2* in maintenance of mitotic fidelity and genomic integrity.

Results

Expression of mammalian warts/lats homologues during embryogenesis

Murine *Lats1* and *Lats2* embryonic expression was examined by Northern analysis and *in situ* hybridization of whole-mount and sectioned embryo specimens. *Lats1* and *Lats2* expression appeared equivalent throughout development (embryonic days (E) 7–17) by Northern analysis (Figure 1A–C); however, *in situ* hybridization revealed a disparity in the spatial distribution of expression (Figure 1D–S). Prominent expression of *Lats1* and *Lats2* was found in tissues of ectodermal and mesodermal origin, respectively. At E8.5–9.5, *Lats1* was highly expressed in the neural tube, head fold neuroepithelium and auditory vesicles (Figure 1D–F), with prominent expression in the mesencephalon at E10.5 (Figure 1G, L and M). *Lats2* was prominent in lateral mesodermal plate, somites and cardiac outflow tract at E8.5 (Figure 1H and I), and in the general heart field (inflow and outflow tracts, ventricle and atrium) by E10.5 (Figure 1R and S). Moderate *Lats2* expression was observed in the head mesenchyme, dorsal aorta area, developing gut, lungs and dermatome of the somites. Overlapping expressions of *Lats1* and *Lats2* were observed in branchial arches and limb buds, as well as the cardiogenic crescent at E8.5.

Targeted disruption of Lats2

To investigate the biological function of *Lats2*, a targeted disruption of *Lats2* was generated in embryonic stem (ES) cells (Figure 2A–D). An insertional strategy was devised to replace serine 371 of Lats2 with an in-frame stop codon followed by an inverted neomycin cassette in order to disrupt translation of the carboxy-terminal kinase domain. Northern analysis revealed the expected loss of the wild-type 6-kb *Lats2* mRNA in homozygous embryos, and the presence of a longer 8-kb *Lats2* mRNA species produced from the targeted allele (Supplementary Figure 1). To ensure success of the targeting strategy, cDNAs (1.6 kb) derived from the start site of translation to the inserted neo sequence of the mutant allele were obtained by RT–PCR from $Lats2^{+/-}$ mouse mRNA. Two cDNA clones were sequenced entirely to verify that the mutant mRNA species contained sequence replacing serine 371 and early stop codons (Figure 2C). Western blot analysis using cellular extract from $Lats2^{-/-}$ MEFs and polyclonal antisera against Lats2 failed to detect the full-length Lats2 protein or any truncated peptide, indicating that the targeting strategy resulted in a null allele (Figure 2D).

Targeted disruption of Lats2 results in embryonic lethality

Analysis of live-born progeny obtained from 129/C57BL/6 F1 heterozygote crosses revealed that Lats2 is essential for the development of viable progeny (Table I). No viable $Lats2^{-/-}$ offspring were recovered at birth (67 wild type, 37%; 116 $Lats2^{+/-}$, 63%; 0 $Lats2^{-/-}$, 0%), and this lethality was independent of strain when outbred in C57BL/6 and ICR backgrounds. Heterozygous mice were phenotypically indistinguishable from wild-type littermates and a cohort of 40 monitored heterozygotes remained disease free following 1 year of observation.

Embryonic lethality of $Lats2^{-/-}$ mice was observed to occur during E10.5–12.5 (Table I). Progeny from $Lats2^{+/-}$ intercrosses developed normally until E8.5; however, $Lats2^{-/-}$ embryos exhibited pleiotrophic developmental defects at E9.5 and thereafter (Figure 2E–H). $Lats2^{-/-}$ embryos were typically smaller or developmentally delayed (Figure 2E and F) and occasionally were found to contain distended, blood-filled pericardia, haemorrhaging in the body or head region (Figure 2G and H), and irregular kinked neural tubes (Table I).

Histological analyses revealed no specific defect in the development of yolk sac, yolk sac blood islands, blood cells, embryonic vascularization, chorionic-allantois fusion, placental vascularization or differentiation (Supplementary Figure 1). Immunohistochemical staining with anti-PECAM did not reveal any defects in blood vessel formation or appearance (Supplementary Figure 1). $Lats2^{-/-}$ embryos expressed normal levels of placental *PPARγ* (Supplementary Figure 2), a placental differentiation marker that can lead to

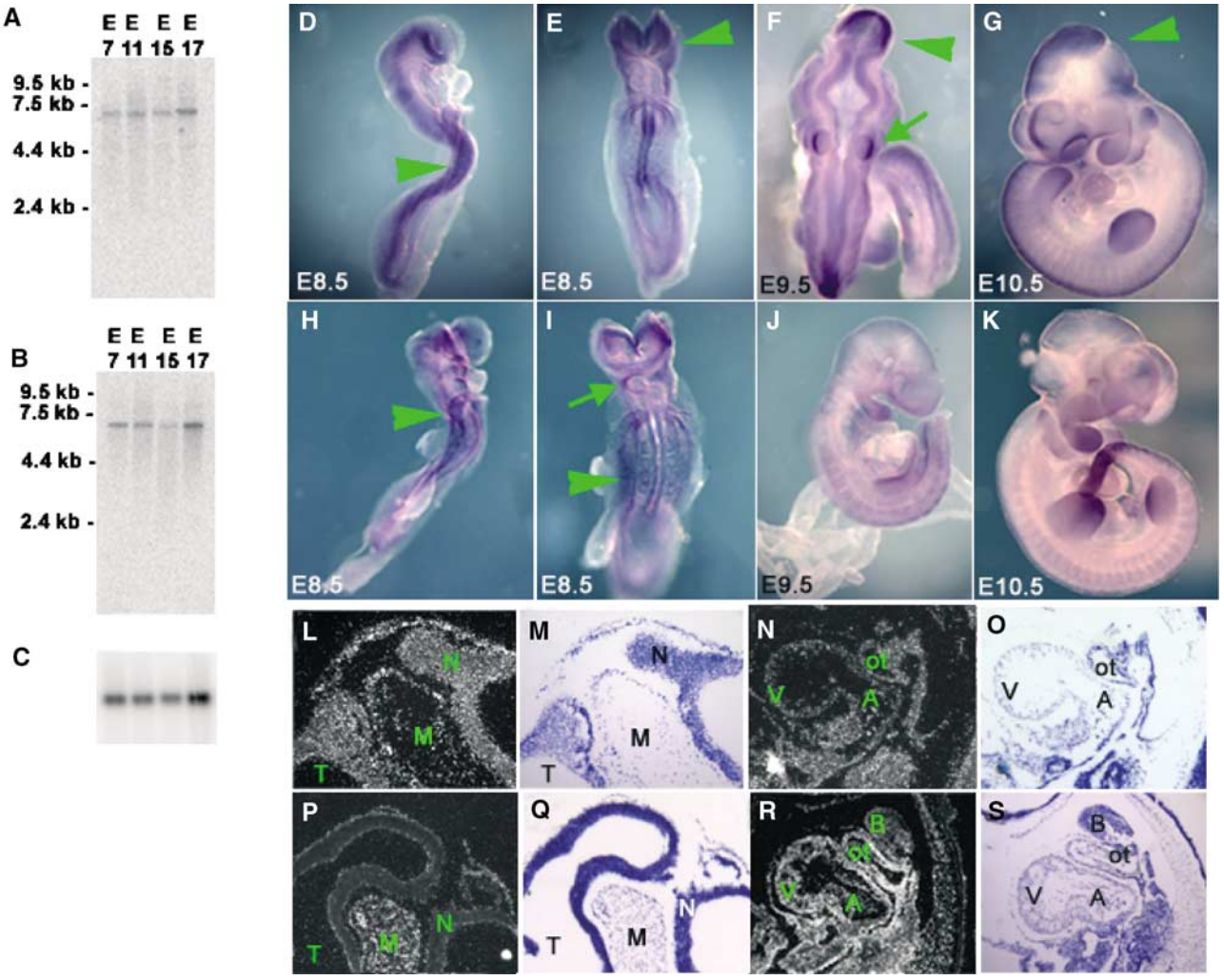

Figure 1 Northern analysis of *Lats1* (**A**) and *Lats2* (**B**) expression during embryonic development. Loading control for Northern blot shown with GADPH (**C**). Whole-mount *in situ* hybridization of *Lats1* (**D–G**) and *Lats2* (**H–K**) during embryonic developmental stages E8.5–10.5. Prominent *Lats1* expression was detected in neuroepithelium (arrows, D, E), mesencephalon (arrows, F, G) and otic vesicles (lower arrow, F), whereas *Lats2* expression was prominent in the lateral mesodermal plate (arrows, H, I) and the cardiac outflow tract (upper arrow, I). *In situ* hybridization (and corresponding counterstaining) of E10.5 embryonic histological sections with *Lats1* (**L–O**) and *Lats2* (**P–S**) showing prominent expression of *Lats1* in neuroepithelium (L, M). *Lats1* expression in the heart (N, O) was relatively lower compared to *Lats2* expression (R, S). N, neuroepithelium; V, ventricle; A, atrium; B, first branchial arch; ot, outflow tract.

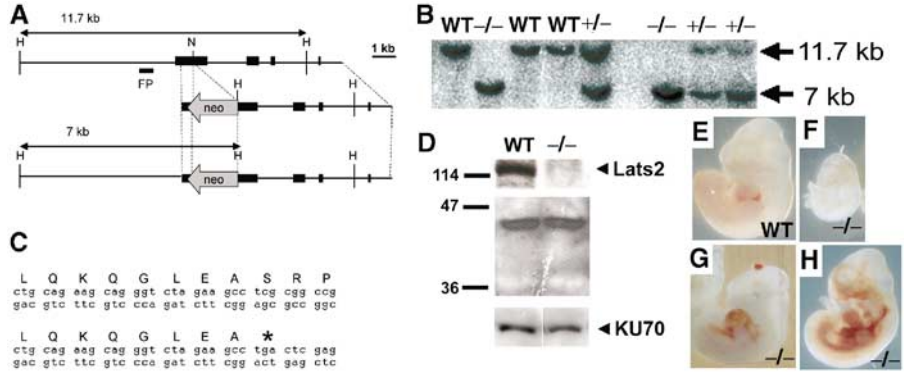

Figure 2 *Lats2* targeted disruption and *Lats2*$^{-/-}$ embryo abnormalities. (**A**) Restriction maps depicting mouse *Lats2* genomic fragment, targeting construct and predicted structure of targeted *Lats2* allele. Exons are represented by filled rectangles. Restriction enzymes: H, *Hin*dIII; N, *Not*I. Digestion of genomic DNA with *Hin*dIII generates an 11.7-kb fragment from the wild-type allele and a 7-kb fragment from the mutant allele, both of which are detected using the 5′ flanking probe shown. (**B**) Southern analysis of genomic DNA extracted from E9.5 embryos obtained from heterozygote crosses. (**C**) Sequence of cDNAs corresponding to *Lats2* mRNA derived from wild-type (upper) and mutant (lower) alleles. (**D**) Western analysis of protein extracts from wild-type and *Lats2*$^{-/-}$ MEFs. Polyclonal antibodies against Lats2 failed to detect full-length protein (upper panel) or a shorter Lats2 peptide (middle panel) in the mutant MEFs. Ku70 is shown as a loading control (lower panel). (**E, F**) Representative E10.5 embryos (photographed at the same magnification as at the time of dissection) depicting reduced size of *Lats2*$^{-/-}$ embryos. (**G, H**) *Lats2*$^{-/-}$ E11.5 embryos with distended pericardium with blood accumulation in the abdominal cavity.

Table I Genotype of progeny collected from *Lats2* heterozygote crosses and classification of $Lat2^{-/-}$defects

Gestational age (days postconception)		Wild type	+/−	−/−	Total typed	Resorptions	Total collected
8.5–8.75	Total	14	22	9	45	0	45
	Viable[a]	14	22	9			
	Dead	0	0	0			
9.0–9.5[b]	Total	38	58	48	144	3	147
	Viable	38	56	46			
	Dead	0	2	2			
10.5[c]	Total	27	43	19	89	2	91
	Viable	27	41	16			
	Dead	0	2	3			
11.5[d]	Total	13	30	18	61	2	63
	Viable	12	30	8			
	Dead	1	0	10			
12.5[e]	Total	10	29	13	52	4	56
	Viable	10	27	1			
	Dead	0	2	12			
Weanling							
129/J × C57BL/6 ($F_1 \times F_1$)		30	56	0	86		
C57BL/6 outbred ($F_2 \times F_2$)		6	11	0	17		
C57BL/6 outbred ($F_3 \times F_3$)		6	8	0	14		
ICR outbred ($F_3 \times F_3$)		25	41	0	66		
Total		67	116	0	183		

[a]At dissection, embryos were determined to be alive based on the presence of a heartbeat.
[b]At E9.5, 25/40 $Lats2^{-/-}$ embryos were either smaller or developmentally delayed compared to wild-type or heterozygous siblings.
[c]At E10.5, $Lats2^{-/-}$ embryos were typically smaller (14/19), delayed in development (2/19) and presented with distended blood-filled pericardia (4/19) and/or haemorrhaging (5/19) in the body/head region.
[d]At E11.5, $Lats2^{-/-}$ embryos were typically smaller (14/18), along with head and/or body cavity haemorrhaging (5/18), a distended and/or blood-filled pericardia (8/18) and irregular kinked neural tubes (5/18).
[e]At E12.5, 12/13 $Lats2^{-/-}$ embryos examined were dead, smaller than littermates, especially in the head (hindbrain/neck), and appeared developmentally arrested at E10.5–11.0.

myocardial thinning due to incomplete placental vascularization if deficient (Barak *et al*, 1999).

Lats2$^{-/-}$ embryos display contrasting defects in cardiac growth

$Lats2^{-/-}$ E9.5 embryos had correctly looped hearts; however, 25% ($n = 12$) contained irregular supernumerary cells invading the interior of the common atrial chamber. The supernumerary cells were primarily located in the myocardium, and extended into the open chamber, with the endocardial layer apparently disrupted (Figure 3A and B). Similar outgrowths were also observed in 33% ($n = 12$) of $Lats2^{-/-}$ E10.5 embryos examined (Figure 3C and D). In contrast, a marked ventricular hypoplasia with defective trabeculae and myocardia was observed in 36% ($n = 14$) of E10.5 $Lats2^{-/-}$ embryos (Figure 3E and F). Cardiac development appeared normal with respect to expression of *cardiac α-actin* (Figure 3G–J), *Bmp4* (Figure 3K–N) and *Nkx2.5* (Supplementary Figure 2). The atrial and ventricular defects, pericardial distension and blood pooling suggest that cardiac insufficiency contributed to embryonic lethality in a subset of $Lats2^{-/-}$ embryos.

Lats2$^{-/-}$ embryos exhibit an arrest in proliferation

Proliferation and apoptosis in embryos were examined using BrdU incorporation and Tdt-mediated dUTP nick end labelling (TUNEL) analysis, respectively. BrdU incorporation was equivalent in E8.5 embryos (Figure 4). However by E9.5, decreased BrdU incorporation was evident in 75% ($n = 12$) of $Lats2^{-/-}$ embryos and by E10.5, all live $Lats2^{-/-}$ embryos examined ($n = 12$) displayed a proliferation defect with respect to decreased (75%) or absent (25%) BrdU incorporation when compared to wild-type and $Lats2^{+/-}$ siblings ($n = 14$). A decreased level of cyclin E was observed in $Lats2^{-/-}$ embryos showing decreased proliferation, while other cyclin levels examined did not differ from the wild-type littermates (Supplementary Figure 3). Despite the proliferation arrest, apoptotic profiles as evaluated by TUNEL analysis and enumeration of DAPI-stained picnotic nuclei were equivalent (Supplementary Figure 4). The proliferation arrest was found to be restricted to the embryonic conceptus, as extraembryonic tissues showed robust BrdU incorporation in $Lats2^{-/-}$ embryos (Supplementary Figure 5). As the decreased BrdU incorporation preceded the appearance of other morphological and histological defects, including the previously described atrial hyperplasia, the proliferation arrest observed is likely responsible for hypoplasia, morphological defects and ultimate lethality in $Lats2^{-/-}$ embryos.

Lats2$^{-/-}$ MEFs display perturbations of growth control

The observed arrest in proliferation during development might be attributed to a cell-intrinsic block in proliferation or the result of perturbed developmental cues. Despite the observed developmental arrest of $Lats2^{-/-}$ *in situ*, we were able to derive and passage MEFs from $Lats2^{-/-}$ E10.5 embryos. A total of three $Lats2^{-/-}$ E10.5 MEF cultures were

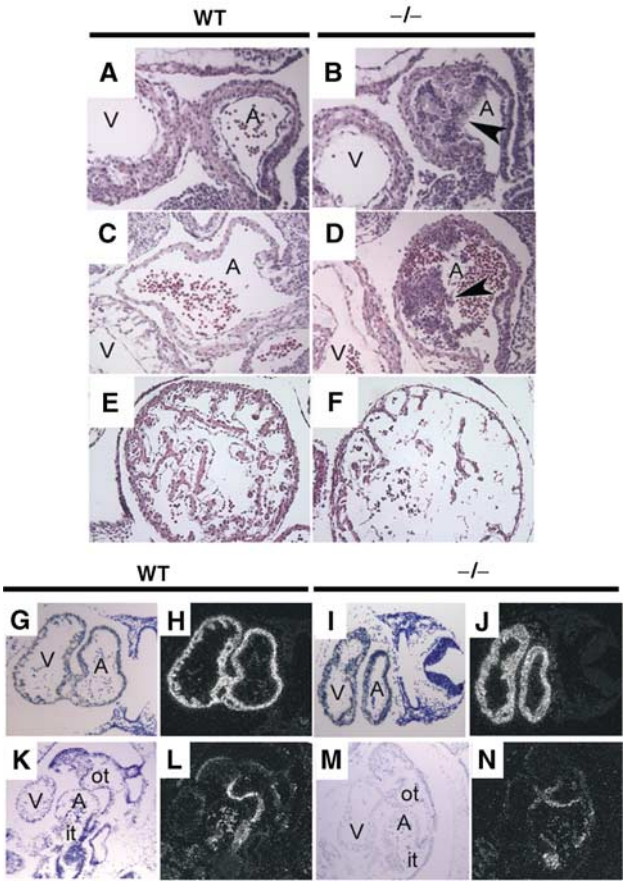

Figure 3 Haematoxylin and eosin-stained sagittal sections of heart (A, atrium; V, ventricle) from wild-type (**A, C**) and mutant (**B, D**) embryos at E9.5 (A, B) and E10.5 (C, D) with atrial hyperplasia (arrows). (**E, F**) Ventricular hypoplasia in *Lats2*$^{-/-}$ embryos. Representative haematoxylin and eosin-stained transverse sections of ventricles from E10.5 wild-type (E) and *Lats2*$^{-/-}$ (F) embryos depicting trabeculation defect and thinner myocardium. Expression of *cardiac actin* at E9.5 (**G–J**) and *Bmp4* at E10.5 (**K–N**) in wild-type (G, H, K, L) and *Lats2*$^{-/-}$ embryos (I, J, M, N) by *in situ* hybridization (A, atrium; V, ventricle; it, inflow tract; ot, outflow tract).

derived and compared to wild-type littermate control cultures. Early passage *Lats2*$^{-/-}$ MEFs showed no impairment in proliferation as assessed by [^{3}H]thymidine incorporation or cell cycle analysis when compared to wild-type littermate cultures of equivalent passage (Supplementary Figure 6). Initial growth rates were comparable to sibling MEF cultures in a standard 3T3 protocol of passage (Figure 5A), but at later passages *Lats2*$^{-/-}$ MEFs grew more rapidly whereas control MEFs entered the expected lag phase of growth. *Lats2*$^{-/-}$ MEFs displayed a greater propensity to achieve a higher saturation density than control MEFs of equivalent passage (Figure 5B). The plating efficiency, as assessed by colony formation of low-passage *Lats2*$^{-/-}$ MEFs, was found to be markedly increased compared to control MEFs of equivalent passage seeded at the same density (Figure 5C). Furthermore, *Lats2*$^{-/-}$ MEFs displayed a partial loss of contact inhibition of growth, as confluent cultures continued to divide and either detach from the culture dish or form foci (Figure 5D–F). Foci were readily stained with crystal violet (Figure 5D) and were composed of rounded and highly refractile cells (Figure 5E and F).

Lats2$^{-/-}$ MEFs display cell division abnormalities

Warts/lats gene family members have homology to gene products that are required for mitotic exit in *S. cerevisiae* and septation in *S. pombe* (Nigg, 2001). As these processes may share common features with cytokinesis in mammalian cells, we investigated the possibility that Lats2 might impact processes that promote separation during cell division. Microscopic examination of wild-type, *Lats2*$^{+/-}$ and *Lats2*$^{-/-}$ MEFs following indirect immunofluorescence of α-tubulin or α-actin revealed that *Lats2*$^{-/-}$ MEFs exhibited an increased propensity (% of cells $\pm$ s.d.) to retain cytoplasmic bridges with neighbouring cells ($35.9 \pm 2.8\%$) compared to wild-type MEFs of equivalent passage ($8.4 \pm 3.6\%$) (Figure 6A–H). During cytokinesis, bundled microtubules that comprise the central spindle form a slender tube called the midbody, which connects the two daughter cells. Successful completion of cytokinesis is dependent on the cleavage of the midbody, a process known as abcission (Glotzer, 2001). The increased retention of cytoplasmic bridges suggests that either *Lats2*$^{-/-}$ MEFs are defective in processes that ensure the correct completion of cytokinesis, or that cytokinesis is impaired by the presence of incorrectly segregated chromatin. In support of the latter possibility, chromatin spanning the midbody of daughter cells could be visualized following immunofluorescent detection of phospho-histone H3 (Figure 6E–G).

Lats2$^{-/-}$ embryos and MEFs display centrosome amplification, multipolar mitotic spindles and genomic instability

Although wild-type MEFs display low levels of genomic instability, especially a propensity to accumulate polyploid cells when passaged (Livingstone *et al*, 1992), we observed a relatively higher frequency (% of cells $\pm$ s.e.m.) of *Lats2*$^{-/-}$ MEFs with micronuclei (Figure 6I–M) ($30.4 \pm 7.2\%$, $n = 3$) compared to wild-type MEF cultures ($8.1 \pm 2.7\%$, $n = 3$). Micronuclei are small extra nuclei within the cytoplasm that represent lagging or damaged chromosomal fragments caused by aberrant mitoses that are excluded from the main daughter nuclei at telophase (Therman and Susman, 1993). *Lats2*$^{-/-}$ cells derived from freshly harvested E10.5 embryos also showed a relatively higher frequency of cells with micronuclei ($38.2 \pm 8.0\%$, $n = 3$) compared to wild-type sibling embryos ($18.6 \pm 4.9\%$, $n = 4$) (Figure 6M). We also evaluated centrosome status in *Lats2*$^{-/-}$ and wild-type freshly harvested embryonic cells and cultured MEFs following γ-tubulin immunostaining. Cells with multiple copies of centrosomes (>2 centrosomes/cell) were rarely observed in wild-type cells, but were frequently observed in *Lats2*$^{-/-}$ embryonic cells (not shown) and early passage MEFs (Figure 6N–S). The frequency of *Lats2*$^{-/-}$ embryonic cells with >2 centrosomes was $56 \pm 14\%$ ($n = 3$, >200 cells scored per embryo) compared to $1.8 \pm 3.7\%$ of wild-type cells ($n = 4$, >200 cells scored per embryo) (Figure 6V). Similarly, the frequency of *Lats2*$^{-/-}$ passage 5 MEFs with >2 centrosomes was 34% ($n = 314$) and 48% ($n = 319$) in two independent lines compared to 5% ($n = 316$) and 3% ($n = 307$) in two independent wild-type lines of equivalent passage (Figure 6V). Functional supernumerary centrosomes might be expected to facilitate multipolar spindle formation during mitosis, leading to suboptimal chromosome segregation and aneuploidy induction. A subset of *Lats2*$^{-/-}$ MEF mitotic

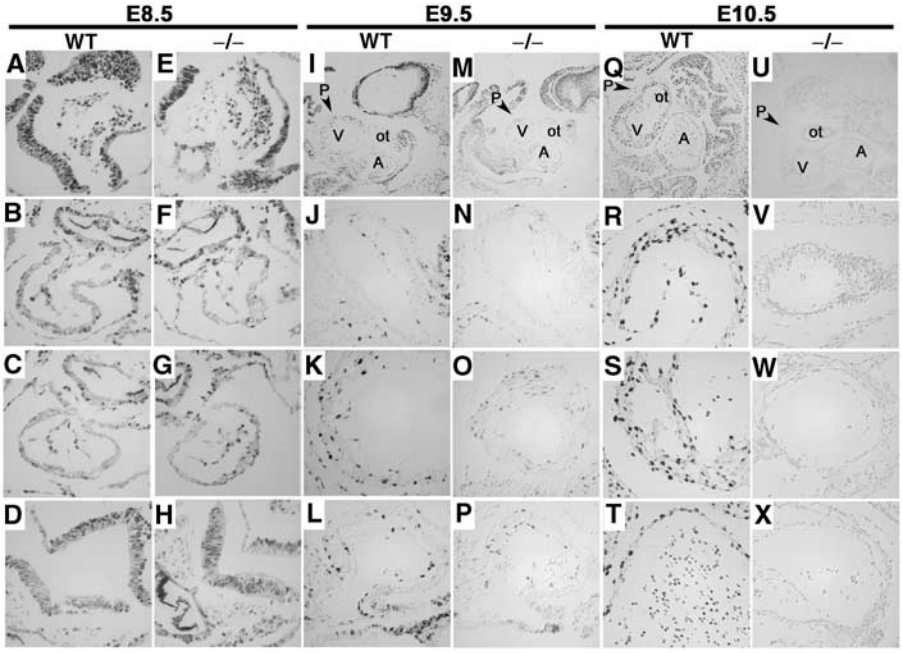

Figure 4 Stage-specific proliferation defect in *Lats2*$^{-/-}$ embryos. E8.5 transverse, E9.5 sagittal and E10.5 sagittal embryo sections stained for BrdU. All images for a given embryonic stage were captured at the same exposure settings and $\times 40$ magnification, unless otherwise stated. (**A, E**) Left side of head fold. (**B, F**) Heart outflow tract. (**C, G**) Heart ventricle. (**D, H**) Neural tube. Top panels for E9.5 and E10.5 depict heart area at $\times 10$ magnification (V, ventricle; A, atrium; ot, outflow tract; P, pericardium) with representative outflow tract (**J, N, R, V**) heart ventricle (**K, O, S, W**) and atrium (**L, P, T, X**) below.

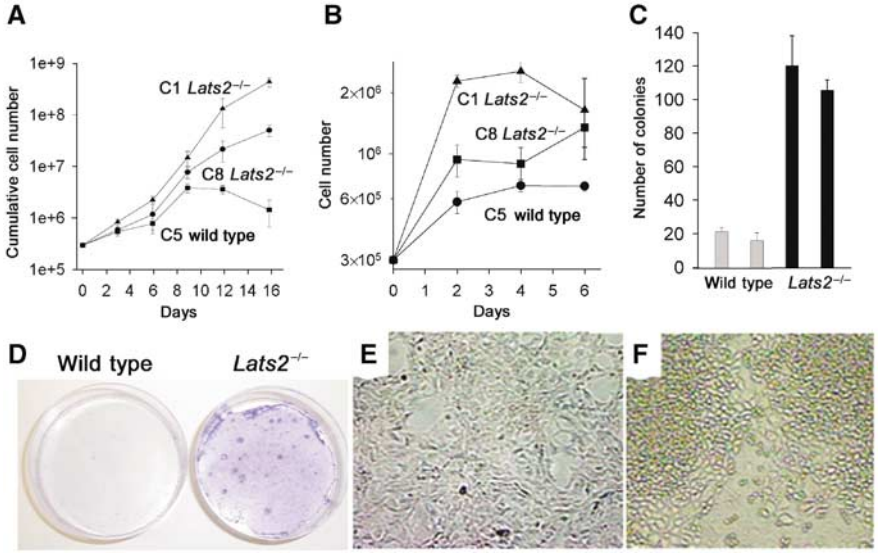

Figure 5 Growth kinetics in *Lats2*$^{-/-}$ MEFs. (**A**) Growth curve representative of passage 2 MEFs derived from wild-type (■) and two independently derived *Lats2*$^{-/-}$ MEF lines (▲ and ●). (**B**) Representative saturation density of growth for passage 2 MEFs derived from wild-type (●) and two independently derived *Lats2*$^{-/-}$ MEF lines (▲ and ■). (**C**) Plating efficiency at low seeding density (colony formation/3000 cells plated) for two wild-type MEF lines (grey bar, $n = 3$) and two *Lats2*$^{-/-}$ MEF lines (black bar, $n = 3$). (**D**) Representative determination of contact inhibition of growth. A total of 5×10^4 cells of either wild-type or *Lats2*$^{-/-}$ MEFs were plated in 6 cm dishes. Cells were maintained in culture without passage for 2 weeks and stained with crystal violet. (**E, F**) Morphology of wild-type MEFs (E) and foci observed in *Lats2*$^{-/-}$ MEFs (F).

events in asynchronous culture (Figure 6T and U) exhibited multipolar mitotic spindles that were not observed in wild-type mitotic cells.

To more rigorously assess alterations in genome integrity, we conducted karyotypic analyses on *Lats2*$^{-/-}$ and wild-type littermate control MEF cultures of equivalent passage. As expected, a substantial number of wild-type MEFs showed loss of diploidy with approximately 56% of wild-type MEFs exhibiting tetraploidy or polyploidy (Figure 6W). In contrast, only 7% of *Lats2*$^{-/-}$ MEFs at the same passage were diploid. *Lats2*$^{-/-}$ MEFs displayed a nearly four-fold increase in the number of aberrant cells containing one or more structural chromosome rearrangements (chromosome/chromatid breaks, double minutes and centromeric fusions) and defects in chromatin condensation at mitosis. The association of Lats2 deficiency with genomic instability was not restricted

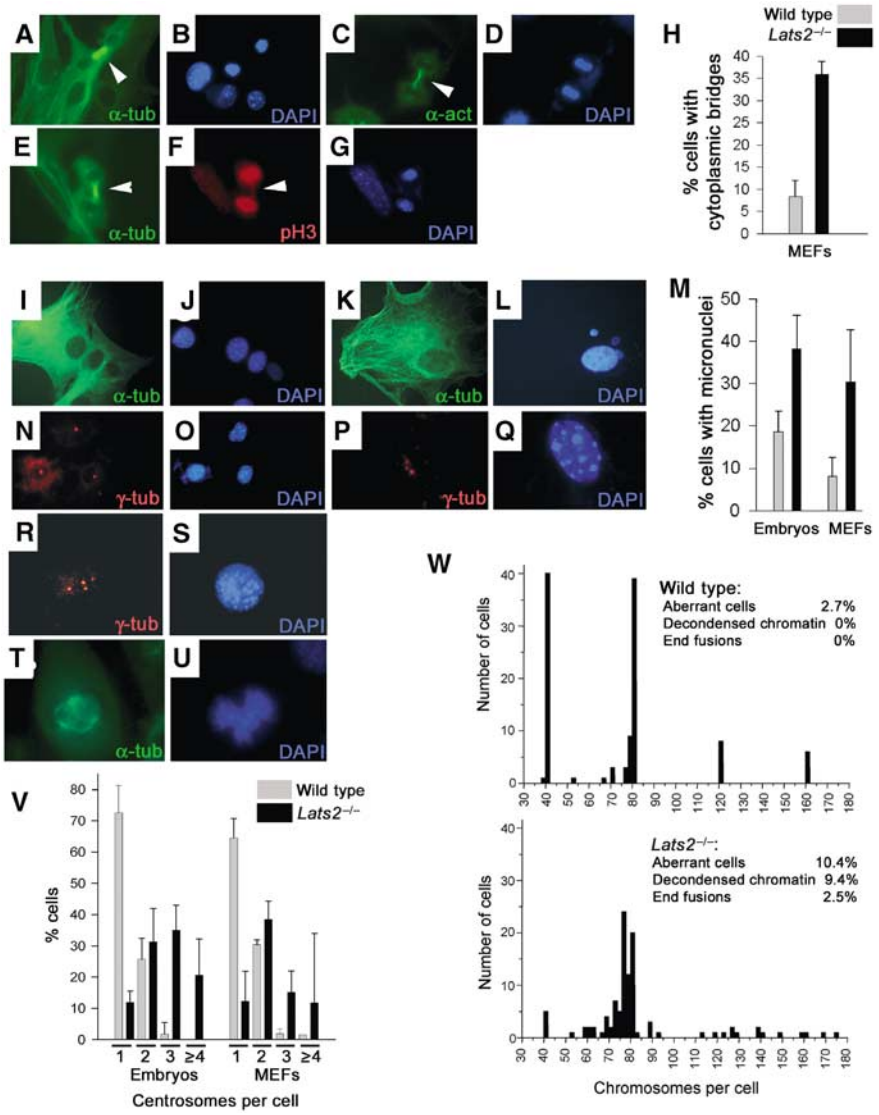

Figure 6 Cytokinesis abnormalities, micronuclei, aneuploidy and centrosome amplification in *Lats2*$^{-/-}$ embryos and MEFs. (**A, B**) *Lats2*$^{-/-}$ MEFs stained with FITC-conjugated anti-α-tubulin to visualize tubulin cytoskeleton (A) with microtubule bundles (arrowhead) and counterstained with DAPI (B) to visualize DNA. (**C, D**) *Lats2*$^{-/-}$ MEFs stained with anti-α-actin (C) and counterstained with DAPI (D) to visualize midbody (arrowhead) and DNA, respectively. (**E–G**) Bridged chromatin within the midbody (E, arrowhead) of *Lats2*$^{-/-}$ MEFs could be detected following staining for phospho-histone H3 (F, arrowhead) (DAPI counterstain shown in G). (**H**) Graph depicting the percentage of cells exhibiting cytoplasmic bridges from three independently derived *Lats2*$^{-/-}$ MEF lines (black bar) compared to three independent wild-type or heterozygous lines of equivalent passage (grey bar). Representative photomicrographs of wild-type MEFs (**I**) with normal nuclear morphology (**J**) and a *Lats2*$^{-/-}$ MEF (**K**) containing micronuclei (**L**) are depicted. (**M**) Graph depicting the percentage of cells exhibiting micronuclei from three wild-type (left grey bar) and *Lats2*$^{-/-}$ (left black bar) sibling embryos and three independently derived *Lats2*$^{-/-}$ MEF lines (right black bar) compared to three independent wild-type or heterozygous lines of equivalent passage (right grey bar). MEFs (**N–S**) were immunostained with anti-γ-tubulin (red) and counterstained with DAPI (blue) to visualize centrosomes and DNA, respectively. Three wild-type MEFs are depicted (N, O) with single centrosomes. *Lats2*$^{-/-}$ MEFs containing three centrosomes (P, Q) and four centrosomes (R, S) are depicted. (**T, U**) Abnormal spindle pole formation and chromosomal segregation defects during mitosis in *Lats2*$^{-/-}$ fibroblasts. Fibroblasts were immunostained with anti-α-tubulin (green) to visualize mitotic spindles and counterstained with DAPI (blue) to visualize chromatin. (**V**) Graph depicting the percentage of cells exhibiting 1, 2, 3 or ⩾4 centrosomes from three wild-type (grey bar) and *Lats2*$^{-/-}$ (black bar) sibling embryos and three independently derived *Lats2*$^{-/-}$ MEF lines (black bar) compared to three independent wild-type or heterozygous lines of equivalent passage (grey bar). (**W**) Pooled results of karyotypic analyses of wild-type MEF lines (upper panel) compared to *Lats2*$^{-/-}$ MEF lines (lower panel) with frequencies of specific chromosomal aberrations observed.

to MEFs, as embryonic cells arrested *in vivo* showed a similar increase in the propensity to accumulate altered chromosome numbers (Supplementary Figure 7).

Lats2 is a centrosomal protein that negatively regulates centrosome duplication

As Lats2-deficient cells exhibited an increased propensity to contain supernumerary centrosomes, we sought to directly assess the relationship of this protein with centrosomes. Due to the lack of a specific antibody against Lats2, we compared the cellular localization of GFP-tagged Lats2 to GFP alone in wild-type MEFs following 24 h after transfection with the respective expression vectors. Cells transfected with *GFP* vector alone demonstrated no specific localization of GFP fluorescence (Figure 7A–C). In contrast, cells transfected with a *GFP-Lats2* expression construct demonstrated GFP

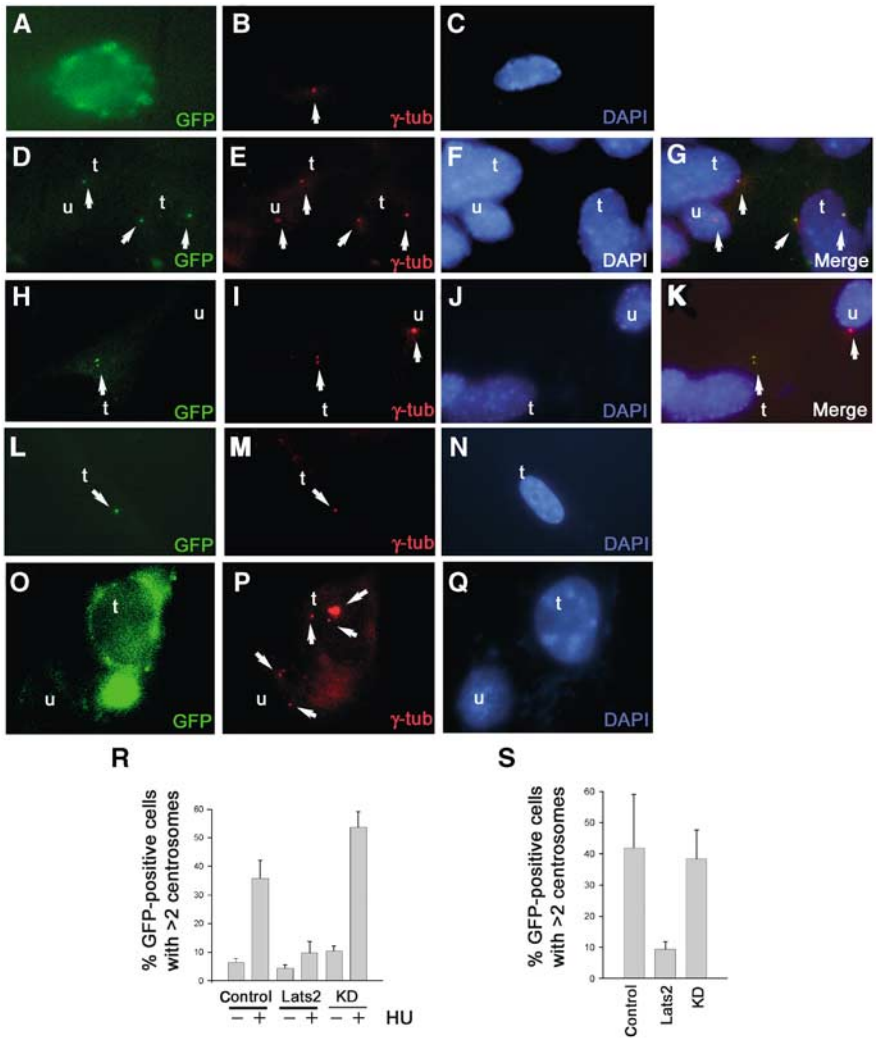

Figure 7 Lats2 is a centrosomal protein that suppresses centrosome overduplication. (**A–K**) Subcellular localization of GFP-Lats2 at centrosomes by indirect immunofluorescence. Wild-type MEFs transfected with either *GFP* (A–C), *GFP-Lats2* (D–K) or *GFP-Lats2KD* (**L–N**) expression constructs were analysed 24 h later for GFP fluorescence (A, D, H, L) and γ-tubulin (red) immunofluorescence (B, E, I, M), and DNA was stained with DAPI (C, F, J, N). Merged images G and K confirming colocalization of GFP-Lats2 and γ-tubulin are derived from (D–F) and (H–J), respectively. Transfected cells (GFP-positive) and untransfected cells in (D–N) are denoted as t and u respectively; arrows indicate centrosomes (B, E, I, M, **P**), GFP-Lats2 fluorescence (D, H), GFP-Lats2KD fluorescence (L) and merged signals (G, K). (**O–Q**) Centrosome overduplication in the presence of HU is suppressed by GFP-Lats2. Representative *GFP* vector-transfected cell (t) and untransfected (u) cell (O) demonstrating supernumerary centrosomes (arrows) as visualized by γ-tubulin immunostaining (P). DNA is visualized by DAPI stain (Q). (**R**) Graph depicting the percentage of GFP-positive cells exhibiting >2 centrosomes from wild-type MEFs transfected with *GFP vector*, *GFP-Lats2* (Lats2) or *GFP-LatsKD* (KD) in the absence or presence of 2 mM HU. (**S**) Centrosome overduplication in *Lats2*-deficient MEFs is suppressed by GFP-Lats2. Graph depicting the percentage of GFP-positive cells exhibiting >2 centrosomes from Lats2$^{-/-}$ MEFs transfected with *GFP* (control), *GFP-Lats2* (Lats2) or *GFP-Lats2KD* (KD).

fluorescence almost exclusively restricted to one or two punctate dots per cell that were found to colocalize with centrosomes stained with anti-γ-tubulin (Figure 7D–K). In order to ascertain whether the kinase activity of Lats2 was required for centrosome localization, we transfected cells with a *GFP-Lats2* expression construct mutated to ablate the kinase activity as previously described (*GFP-Lats2KD,* see Materials and methods). Cells transfected with *GFP-Lats2KD* also contained punctate staining that colocalized with anti-γ-tubulin, indicating that kinase activity was not required for centrosome localization (Figure 7L–N).

Given that GFP-Lats2 localizes to centrosomes, we sought to determine whether Lats2 directly impacts centrosome replication. Centrosome duplication initiates at the G1/S transition in mammalian cells, and is completed during S phase (Doxsey, 2001; Hinchcliffe and Sluder, 2001; Lange, 2002; Nigg, 2002). Under experimental conditions that impose a prolonged S-phase arrest in mammalian somatic cells, multiple rounds of centrosome duplication are facilitated in the absence of DNA replication or cytokinesis (Balczon *et al*, 1995). Using a previously described centrosome duplication assay (Meraldi *et al*, 1999), we investigated whether overexpression of GFP-Lats2 would suppress centrosome reduplication in wild-type MEFs following treatment with hydroxyurea (HU), an agent that facilitates S-phase arrest. HU treatment of cells transfected with *GFP* (Figure 7O–Q) resulted in a higher frequency of cells exhibiting three or more centrosomes per cell (35.8±6.3%, mean±s.d. of three

experiments) compared to transfected cells without HU treatment (6.4±1.4%) as expected (Figure 7R). In contrast, HU-treated cells transfected with *GFP-Lats2* showed a suppression of centrosome reduplication (9.8±4.0%) (Figure 7R). A requirement for the kinase activity of Lats2 in the suppression of centrosome reduplication was observed, in that HU-treated cells transfected with *GFP-Lats2KD* exhibited a higher frequency of cells exhibiting three or more centrosomes per cell (53.7±5.5%) compared to transfected cells without HU treatment (10.4±1.8%) (Figure 7R).

We then sought to determine whether expression of GFP-Lats2 would be sufficient to suppress the centrosome overduplication phenotype inherent in *Lats2*$^{-/-}$ MEFs. Lats2-deficient MEFs transfected with *GFP-Lats2* were found to exhibit a lower frequency of cells with three or more centrosomes (9.4±2.4% of GFP-positive cells, mean±s.d. of three experiments) compared to Lats2-deficient MEFs transfected with *GFP* alone (41.8±17.1%). In contrast, expression of GFP-Lats2KD in Lats2-deficient MEFs did not suppress the frequency of cells with supernumerary centrosomes (38.4±9.1%), implicating Lats2 kinase activity in mediating the suppression of the centrosome overduplication phenotype (Figure 7S). These results support a role for Lats2 in maintenance of normal centrosome copy number through negative regulation of centrosome overduplication.

Discussion

Distinct requirements for mammalian warts/lats orthologues in embryonic development

The spatial disparity in embryonic expression that is especially apparent at E8.5 indicates that *Lats1* and *Lats2* might play specialized roles in the development of tissues of ectodermal and mesodermal origin, respectively. The observed embryonic lethality in *warts/lats* mutant flies contrasted with the perinatal lethality observed in a majority of *Lats1*$^{-/-}$ mice (St John *et al*, 1999). Our study demonstrates that the developmental requirements for *Lats1* and *Lats2* are strikingly different, in that *Lats2* is essential for development before E12.5. Hence the embryonic expression patterns observed together with the embryonic requirement for Lats2 in contrast to Lats1 suggest that mammalian *warts/lats* orthologues are required during distinct developmental stages.

Differential requirements for Lats2 in developmental versus cell-intrinsic control of proliferation

The mesodermal prominence of *Lats2* expression, together with the observed defects in cell growth control in *lats/warts* mutant flies, led to the expectation of lineage-restricted overproliferation in *Lats2*$^{-/-}$ mice. However, cellular hyperplasia was only observed to occur in a subset of *Lats2*$^{-/-}$ embryos, and was only noted in the atrial chamber of the developing heart. Furthermore, these observations contrasted to the marked ventricular hypoplasia observed in a number of embryos. These findings suggest differential requirements for Lats2 in atrial versus ventricular growth in the embryonic heart, and may explain the cardiac insufficiency observed in *Lats2*$^{-/-}$ embryos. However, the predominant defect that preceded embryonic lethality was a progressive arrest in proliferation.

The proliferation arrest in *Lats2*$^{-/-}$ embryos, but not in MEFs, indicates that Lats2 facilitates essential processes for developmental stage-specific cell cycle progression (Vidwans and Su, 2001). *Lats2*$^{-/-}$ early passage MEFs were indistinguishable from wild-type littermate control MEFs with respect to morphology, proliferation and analysis of cell cycle profiles. However, upon further passage, *Lats2*$^{-/-}$ MEFs bypass culture-induced replicative arrest and fail to exhibit the expected slow-growth phase. Normal MEFs typically arrest in response to contact inhibition of growth. Proliferation control in *Lats2*$^{-/-}$ MEFs exhibited less dependence on contact inhibition in that *Lats2*$^{-/-}$ MEF monolayers achieved higher cellular densities and exhibited the propensity to form focal overgrowths at saturated densities. These properties are strikingly reminiscent of the cell-autonomous overproliferation phenotypes observed in *Drosophila* with mutations in *warts/lats* (Bryant *et al*, 1993; Justice *et al*, 1995; Xu *et al*, 1995).

Impact of Lats2 on centrosome duplication and genomic integrity

Both *Lats2*$^{-/-}$ embryos and MEFs were found to exhibit propensities for centrosome amplification and genomic instability. The increased prevalence of centrosome amplification and genomic instability observed in *Lats2*$^{-/-}$ embryos and MEFs suggests that Lats2 is required to maintain correct chromosomal segregation. The subcellular localization of Lats2 to centrosomes strongly implies a role for this protein in centrosome function. Furthermore, the ability of GFP-Lats2 to suppress centrosome reduplication in the presence of HU and reverse the centrosome amplification inherent in *Lats2*$^{-/-}$ MEFs directly supports a role for this protein in a cell cycle checkpoint that regulates centrosome duplication.

Centrosomes normally replicate only once during each round of cell division, beginning near the G1/S transition and finishing by G2 phase (Doxsey, 2001; Lange, 2002). During mitosis, centrosomes facilitate the correct segregation of mitotic chromosomes through the formation of a bipolar spindle. Several studies have identified mammalian factors that regulate centrosome duplication (Meraldi *et al*, 1999; Okuda *et al*, 2000; Fisk and Winey, 2001; Chen *et al*, 2002). The acquisition of supernumerary centrosomes and generation of multipolar spindles during mitosis would be expected to generate conditions that facilitate the unequal segregation of chromosomes and genomic instability (Doxsey, 2001; Glotzer, 2001; Lange, 2002; Nigg, 2002). The increased prevalence of micronuclei, chromosomal defects and aneuploidy of *Lats2*$^{-/-}$ embryos and MEFs is symptomatic of structural chromosomal aberrations that result in unequal segregation of chromosomes during cell division.

It is unclear whether the impaired cytokinesis in Lats2-deficient cells is directly caused by deregulated centrosome duplication, or whether Lats2 plays an independent role in this process. A study that analysed centrosome movement in living cells during cytokinesis suggests a requirement for centrosomes in facilitating cell separation (Piel *et al*, 2001); however, this finding is seemingly incompatible with observations that cytokinesis proceeds to completion in cells following laser-mediated ablation of centrosomes (Khodjakov *et al*, 2000). As *Lats2*$^{-/-}$ MEFs display a propensity to exhibit loss of contact inhibition of growth and defects in cell division, it is tempting to speculate that Lats2 may act as a conduit in processes linking contact inhibition of growth with cell division.

Defects in centrosome copy number, cytokinesis and the aneuploidy associated with *Lats2* mutation might contribute to the impaired embryonic proliferation. Embryonic requirements for proper centrosome duplication and cytokinesis might be expected to be more stringent than for cells in culture, as centrosome-dependent pathways would be expected to impact spatial controls that govern the formation of bipolar spindles, thereby determining the plane of cell division during development (Vidwans and Su, 2001).

A potential role for Lats2 in tumour suppression

The *warts/lats* gene family confers tumour suppressor activity both in vertebrates (St John *et al*, 1999) and invertebrates (Bryant *et al*, 1993; Justice *et al*, 1995; Xu *et al*, 1995). Interestingly, Lats2 deficiency was found to impair cytokinesis, promote the accumulation of supernumerary centrosomes and genomic instability. Supernumerary centrosomes and multipolar mitotic spindles have been predicted to contribute to aneuploidy and cancer development (Lingle and Salisbury, 2000); however, it remains to be shown whether centrosome amplification is a cause or a consequence of aneuploidy (Doxsey, 2001; Lange, 2002; Nigg, 2002). An imbalance in chromosomal partitioning might facilitate the emergence of cells defective in various aspects of proliferation control observed. Subsequent cell divisions in the presence of unbalanced centrosome numbers would then be expected to contribute to the chromosome mis-segregation and the generation of aneuploid cell populations. Increased number of micronuclei in *Lats2*$^{-/-}$ cells might indicate the loss of whole chromosome(s) or chromosomal regions as these are eliminated from the cells as micronuclei during subsequent cell division (Therman and Susman, 1993).

Previous studies have implicated *warts/lats* family members as tumour suppressors; however, the underlying mechanisms remain unclear. Although mammalian Lats1/h–Warts-1 has been found to be associated with Cdk1, a direct link between tumorigenesis in *Lats1/Warts-1*-deficient mice and loss of Cdk1 control is unclear. Furthermore, the deregulation of Cdk1 activity as a mechanism sufficient to explain the excessive cell proliferation in *Drosophila warts/lats* mutants has been questioned (Weinkove and Leevers, 2000; Tapon *et al*, 2002). *Lats2*$^{-/-}$ embryonic lethality presently impedes direct evaluation of *Lats2* as a tumour suppressor; however, the bypass of replicative arrest and loss of contact inhibition in MEFs provide direct evidence for a conserved role of *Lats2* in processes linked to proliferation control. Furthermore, we demonstrate that Lats2 deficiency promotes genomic instability. The localization of Lats2 to centrosomes and its role as a negative regulator of centrosome copy number is supportive of a role for centrosome amplification as a process that facilitates genomic instability.

Materials and methods

Northern analysis and in situ hybridization

Northern blot analysis was performed with embryonic RNA blots (Clontech) using *Lats1* and *Lats2* cDNAs as probes. Whole-mount embryo *in situ* hybridization was performed as described previously (Bruneau *et al*, 2001). *In situ* hybridization of embryonic tissue sections was performed using ^{33}P-labelled RNA probes specific for *Lats1*, *Lats2*, *cardiac actin*, *Nkx2.5*, *PPARγ*, and *Bmp4* according to standard methodology.

Targeted disruption of Lats2

A targeting strategy by use of homologous recombination in E14K ES cells was devised to create an insertional mutation resulting in the disruption of downstream kinase domains of *Lats2*. The targeting vector contained the *neomycin* gene flanked by a 0.6-kb upstream homologous region and a 6.0-kb downstream homologous region. The upstream homology short arm sequence was modified to replace sequence encoding serine 371 with a stop codon, thereby disrupting translation of the downstream carboxy-terminal kinase domain. G418-resistant ES clones were screened for homologous recombination by PCR using primers 5′-CCCAGGCT CACCAGCATCCTC-3′ and 3′-CTCACCCTCCTTACTCGACCGG-5′. Correctly targeted ES cells were further verified by Southern analysis. Four *Lats2* heterozygote ES cell lines were injected into C57BL/6 blastocysts and transferred to pseudopregnant ICR females. Germline transmission was verified using Southern analysis. Genotyping of DNA isolated from ES cells, mouse tails or yolk sacs was performed by PCR using primers 5′-CGCCACCA GATGCCTATTCCA-3′ and 3′-ACCTCTGCTTCCTCCCGTCG-5′ (wild type) or primers 5′-CCCAGGCTCACCAGCATCCTC-3′ and 3′-CTCACCCTCCTTACTCGACCGG-5′ (mutant). Western blots of protein from wild-type and *Lats2*$^{-/-}$ MEFs were performed using affinity-purified antisera raised against Lats2 aa 255–273 (YGVQRSSSFQNKTPPDAYS).

Histological analysis, BrdU incorporation, TUNEL analysis and immunohistochemistry

Mouse embryos were fixed, dehydrated and processed according to standard protocols. Embryonic vascularization was analysed with anti-PECAM immunostaining. Placental differentiation was analysed by placental PPARγ expression (Barak *et al*, 1999). Pregnant mice were injected with 0.1 mg BrdU/g mouse weight intraperitoneally 45 min prior to collecting embryos. Sections of embryos were immunostained for BrdU as described previously (Hakem *et al*, 1998). TUNEL staining was performed on histological sections using an *in situ* cell death detection kit (Boehringer Mannheim).

Analysis of embryonic cells and derivation of embryonic fibroblasts

E10.5 embryos (judged to be alive by visual confirmation of cardiac contractions) were harvested, trypsinized and seeded in αMEM media with 10% fetal bovine serum. For immunostaining of embryonic cells, freshly trypsinized embryos were seeded on coverslips coated with poly-L-lysine and processed as described below. Initial MEF cultures were obtained in 6 cm dishes and considered at passage 0 prior to dilution. For growth curves, 3×10^5 cells/6 cm dish at passage 2 were plated and counted, before dilution to 3×10^5 cells/dish for the next passage. For saturated density of growth, 3×10^5 cells/6 cm dish at passage 2 or 3 were plated, counted and replated without dilution on the indicated days. For colony formation assays, 3×10^3 cells/6 cm dish were seeded and the number of colonies formed was enumerated. Immunostaining was performed on cells according to standard methodology with either anti-α-tubulin (FITC-conjugated, Sigma), anti-actin (Sigma), anti-phospho-histone H3 (Upstate Biotechnologies) or anti-γ-tubulin (Sigma), followed by TRITC-conjugated donkey anti-mouse or anti-rabbit secondary IgG (Jackson). Centrosomes were enumerated in cells from three pairs of wild-type or *Lats2*$^{-/-}$ sibling embryos as well as two independently derived *Lats2*$^{-/-}$ and wild-type MEF lines from sibling embryos at passage 5 following γ-tubulin immunostaining.

MEF transfection and centrosome duplication assays

A full-length *Lats2* cDNA cloned from a mouse cDNA library (Origene) was modified by PCR to facilitate ligation into pEGFP-C2 (Clontech) as an *Eco*RI–*Xho*I fragment fused in-frame with the *GFP* coding sequence. A kinase-inactive mutant of Lats2 was created by PCR (as described in Hori *et al*, 2000) and inserted into pEGFP-C2 fused in-frame with GFP coding sequence. Wild-type or *Lats2*$^{-/-}$ MEFs were seeded onto coverslips in six-well tissue culture dishes and DNA constructs were transfected using Lipofectamine PLUS (Invitrogen/Life Technologies). At 3 h after transfection, cells were treated with HU (Sigma) at a final concentration of 2 mM for 36 h and processed for indirect immunofluorescence as described previously. Quantitative analysis of centrosome numbers was performed on 200–600 GFP-positive cells/transfection and each transfection was replicated in at least three separate experiments.

Karyotyping analysis

Mitotic MEFs were collected following colcemid treatment and processed by standard cytogenetic procedures. Slides were stained with DAPI (Sigma) and chromosome number and gross chromosomal rearrangements were determined in 50 metaphase cells per sample from each genotype (two samples per genotype were used). For *in vivo* studies, pregnant females were injected with colcemid (5 μg) 1 h prior to harvesting. E9.5 embryos were isolated and used to prepare single-cell suspensions, which were incubated with colcemid (100 ng/ml) for 4 h at 37°C. Cells were then processed by standard cytogenetic procedures.

Supplementary data

Supplementary data are available at *The EMBO Journal* Online.

Acknowledgements

We thank J Rossant, M Soengas and J de la Pompa for reviewing the manuscript, JM Roberts and A Jurisicova for helpful advice, and D Bouchard and A Wakeham for technical support. JPM was supported by a fellowship from the Canadian Institute of Health Research. This work was supported by Amgen Inc. and by grants from the Canadian Institute of Health Research and the National Cancer Institute of Canada to RH. BGB is supported by the Canadian Institute of Health Research and the Heart and Stroke Foundation of Ontario. MPH acknowledges the grant support from Academic Research Fund and Oncology Research Institute (OLS), National University of Singapore.

References

Andreassen PR, Lohez OD, Lacroix FB, Margolis RL (2001) Tetraploid state induces p53-dependent arrest of nontransformed mammalian cells in G1. *Mol Biol Cell* **12:** 1315–1328

Balczon R, Bao L, Zimmer WE, Brown K, Zinkowski RP, Brinkley BR (1995) Dissociation of centrosome replication events from cycles of DNA synthesis and mitotic division in hydroxyurea-arrested Chinese hamster ovary cells. *J Cell Biol* **130:** 105–115

Barak Y, Nelson MC, Ong ES, Jones YZ, Ruiz-Lozano P, Chien KR, Koder A, Evans RM (1999) PPARγ is required for placental, cardiac, and adipose tissue development. *Mol Cell* **4:** 585–595

Borel F, Lohez OD, Lacroix FB, Margolis RL (2002) Multiple centrosomes arise from tetraploidy checkpoint failure and mitotic centrosome clusters in p53 and RB pocket protein-compromised cells. *Proc Natl Acad Sci USA* **99:** 9819–9824

Brinkley BR (2001) Managing the centrosome numbers game: from chaos to stability in cancer cell division. *Trends Cell Biol* **11:** 18–21

Bruneau BG, Bao ZZ, Fatkin D, Xavier-Neto J, Georgakopoulos D, Maguire CT, Berul CI, Kass DA, Kuroski-de Bold ML, de Bold AJ, Conner DA, Rosenthal N, Cepko CL, Seidman CE, Seidman JG (2001) Cardiomyopathy in Irx4-deficient mice is preceded by abnormal ventricular gene expression. *Mol Cell Biol* **18:** 5099–5108

Bryant PJ, Watson KL, Justice RW, Woods DF (1993) Tumour suppressor genes encoding proteins required for cell interactions and signal transduction in *Drosophila*. *Dev Suppl* **1:** 239–249

Chen Z, Indjeian VB, McManus M, Wang L, Dynlacht BD (2002) CP110, a cell cycle-dependent CDK substrate, regulates centrosome duplication in human cells. *Dev Cell* **3:** 339–350

Doxsey S (2001) Re-evaluating centrosome function. *Nat Rev Mol Cell Biol* **2:** 688–698

Fisk HA, Winey M (2001) The mouse Mps1p-like kinase regulates centrosome duplication. *Cell* **106:** 95–104

Galipeau PC, Cowan DS, Sanchez CA, Barrett MT, Emond MJ, Levine DS, Rabinovitch PS, Reid BJ (1996) 17p (p53) allelic losses, 4*N* (G2/tetraploid) populations, and progression to aneuploidy in Barrett's esophagus. *Proc Natl Acad Sci USA* **93:** 7081–7084

Glotzer M (2001) Animal cell cytokinesis. *Annu Rev Cell Dev Biol* **17:** 351–386

Hakem R, Hakem A, Duncan GS, Henderson JT, Woo M, Soengas MS, Elia A, de la Pompa JL, Kagi D, Khoo W, Potter J, Yoshida R, Kaufman SA, Lowe SW, Penninger JM, Mak TW (1998) Differential requirement for caspase 9 in apoptotic pathways *in vivo*. *Cell* **94:** 339–352

Hartwell LH, Kastan MB (1994) Cell cycle control and cancer. *Science* **266:** 1821–1828

Hinchcliffe EH, Sluder G (2001) 'It takes two to tango': understanding how centrosome duplication is regulated throughout the cell cycle. *Genes Dev* **15:** 1167–1181

Hirota T, Morisaka T, Nishiyama Y, Marumoto T, Tada K, Hara T, Masuko N, Inagaki M, Hatakeyama K, Saya H (2000) Zyxin, a regulator of actin filament assembly, targets the mitotic apparatus by interacting with h-warts/LATS1 tumour suppressor. *J Cell Biol* **149:** 1073–1086

Hori T, Takaori-Kondo A, Kamikubo Y, Uchiyama T (2000) Molecular cloning of a novel human protein kinase, kpm, that is homologous to warts/lats, a *Drosophila* tumor suppressor. *Oncogene* **19:** 3101–3109

Justice RW, Zilian O, Woods DF, Noll M, Bryant PJ (1995) The *Drosophila* tumor suppressor gene warts encodes a homolog of human myotonic dystrophy kinase and is required for the control of cell shape and proliferation. *Genes Dev* **9:** 534–546

Kamikubo Y, Takaori-Kondo A, Uchiyama T, Hori T (2003) Inhibition of cell growth by conditional expression of kpm, a human homologue of *Drosophila* warts/lats2 tumor suppressor. *J Biol Chem* **278:** 17609–17614

Khodjakov A, Cole RW, Oakley BR, Rieder CL (2000) Centrosome-independent mitotic spindle formation in vertebrates. *Curr Biol* **10:** 59–67

Lange BMH (2002) Integration of the centrosome in cell cycle control, stress response and signal transduction pathways. *Curr Opin Cell Biol* **14:** 35–43

Li Y, Pei J, Xia H, Ke H, Wang H, Tao W (2003) Lats2, a putative tumor suppressor, inhibits G1/S transition. *Oncogene* **22:** 4398–4405

Lingle WL, Barrett SL, Negron VC, D'Assoro AB, Boeneman K, Liu W, Whitehead CM, Reynolds C, Salisbury JL (2002) Centrosome amplification drives chromosomal instability in breast tumor development. *Proc Natl Acad Sci USA* **99:** 1978–1983

Lingle WL, Lutz WH, Ingle JN, Maihle NJ, Salisbury JL (1998) Centrosome hypertrophy in human breast tumors: implications for genomic stability and cell polarity. *Proc Natl Acad Sci USA* **95:** 2950–2955

Lingle WL, Salisbury JL (2000) The role of the centrosome in the development of malignant tumors. *Curr Top Dev Biol* **49:** 313–329

Livingstone LR, White A, Sprouse J, Livanos E, Jacks T, Tlsty TD (1992) Altered cell cycle arrest and gene amplification potential accompany loss of wild-type p53. *Cell* **70:** 923–935

Meraldi P, Honda R, Nigg EA (2002) Aurora-A overexpression reveals tetraploidization as a major route to centrosome amplification in p53−/− cells. *EMBO J* **21:** 483–492

Meraldi P, Lukas J, Fry AM, Bartek J, Nigg EA (1999) Centrosome duplication in mammalian somatic cells requires E2F and Cdk2–cyclin A. *Nat Cell Biol* **1:** 88–93

Minn AJ, Boise LH, Thompson CB (1996) Expression of Bcl-xL and loss of p53 can cooperate to overcome a cell cycle checkpoint induced by mitotic spindle damage. *Genes Dev* **10:** 2621–2631

Mitelman F (1971) The chromosomes of fifty primary Rous rat sarcomas. *Hereditas* **69:** 155–186

Nigg EA (2001) Mitotic kinases as regulators of cell division and its checkpoints. *Nat Rev Mol Cell Biol* **2:** 21–32

Nigg EA (2002) Centrosome aberrations: cause or consequence of cancer progression? *Nat Rev Cancer* **2:** 1–11

Nishiyama Y, Hirota T, Morisaki T, Hara T, Marumoto T, Iida S, Makino K, Yamamoto H, Hiraoka T, Kitamura N, Saya H (1999) A human homolog of *Drosophila* warts tumor suppressor, h-warts, localized to mitotic apparatus and specifically phosphorylated during mitosis. *FEBS* **459:** 159–165

Okuda M, Horn HF, Tarapore P, Tokuyama Y, Smulian AG, Chan PK, Knudsen ES, Hofmann IA, Snyder JD, Bove KE, Fukasawa K (2000) Nucleophosmin/B23 is a target of CDK/cyclin E in centrosome duplication. *Cell* **103:** 127–140

Piel M, Nordberg J, Euteneuer U, Bornens M (2001) Centrosome-dependent exit of cytokinesis in animal cells. *Science* **291:** 1550–1553

St John MAR, Tao W, Fei X, Fukumoto R, Carcangi ML, Brownstein DG, Parlow AF, McGrath J, Xu T (1999) Mice deficient of Lats1

develop soft-tissue sarcomas, ovarian tumours and pituitary dysfunction. *Nat Genet* **21:** 182–186

Tao W, Zhang S, Turenchalk GS, Stewart RA, St John MA, Chen W, Xu T (1999) Human homologue of the *Drosophila melanogaster* lats tumour suppressor modulates CDC2 activity. *Nat Genet* **21:** 177–181

Tapon N, Harvey KF, Bell DW, Wahrer DCR, Shiripo TA, Haber DA, Hariharan IK (2002) Salvador promotes both cell cycle exit and apoptosis in *Drosophila* and is mutated in human cancer cell lines. *Cell* **110:** 467–478

Therman E, Susman M (1993) *Human Chromosomes, Structure, Behaviour and Effects*. New York, NY: Springer-Verlag

Vidwans SJ, Su TT (2001) Cycling through development in *Drosophila* and other metazoa. *Nat Cell Biol* **3:** E35–E39

Weinkove D, Leevers SJ (2000) The genetic control of organ growth: insights from *Drosophila*. *Curr Opin Genet Dev* **10:** 75–80

Xu T, Wang W, Zhang S, Stewart RA, Yu W (1995) Identifying tumor suppressors in genetics mosaics: the *Drosophila* lats gene encodes a putative protein kinase. *Development* **121:** 1053–1063

Yabuta N, Fujii T, Copeland NG, Gilbert DJ, Jenkins NA, Nishiguchi H, Endo Y, Toji S, Tanaka H, Nishimune Y, Nojima H (2000) Structure, expression, and chromosome mapping of LATS2, a mammalian homologue of the *Drosophila* tumour suppressor gene lats/warts. *Genomics* **63:** 263–270